Observation of Electron Energies Beyond the Linear Dephasing Limit from a Laser-Excited Relativistic Plasma Wave

D. Gordon,[1] K. C. Tzeng,[1] C. E. Clayton,[1] A. E. Dangor,[2] V. Malka,[3] K. A. Marsh,[1] A. Modena,[2] W. B. Mori,[1] P. Muggli,[1] Z. Najmudin,[2] D. Neely,[4] C. Danson,[4] and C. Joshi[1]

[1]*University of California, Los Angeles, California 90095*

[2]*Imperial College of Science, Technology, and Medicine, London, United Kingdom*

[3]*Ecole Polytechnique, Palaiseau, France*

[4]*Rutherford Appleton Laboratory, Didcot, United Kingdom*

(Received 11 April 1997)

The spatial extent of the plasma wave and the spectrum of the accelerated electrons are simultaneously measured when the relativistic plasma wave associated with Raman forward scattering of an intense laser beam reaches the wave breaking limit. The maximum observed energy of 94 MeV is greater than that expected from the phase slippage between the electrons and the accelerating electric field as given by the linear theory for preinjected electrons. The results are in good agreement with 2D particle-in-cell code simulations of the experiment. [S0031-9007(98)05516-1]

PACS numbers: 52.40.Nk, 41.75.Lx, 52.35.Mw, 52.35.Nx

The systematic understanding of wave-particle dynamics is crucial to the application of relativistically propagating plasma waves as ultrahigh gradient accelerating structures [1]. Within the last five years many significant experimental milestones have been reached in this rapidly advancing field using either the beat-wave scheme [2–4] or the self-modulation scheme [5–7] to excite the plasma wave. These include the acceleration of externally injected electrons [2] as well as self-trapped electrons [3] by such waves, the demonstration of trapping of the externally injected electrons [4] in the potential well of such a wave, acceleration of self-trapped electrons at a maximum possible accelerating gradient [5] determined by "wave breaking," and the extraction of a high current beam of electrons [7] from this latter process. In this Letter we report yet another important milestone: the observation of energies of self-trapped particles which exceed the limit imposed by the phase slippage between the particles and the accelerating electric field as predicted by linear theory.

In the linear, but two dimensional, cold plasma theory, the maximum energy [8] of an electron trapped by the potential of a relativistic plasma wave having an amplitude $e\phi = \epsilon mc^2$ is given in the limit $\epsilon\gamma_{\rm ph} > 1$ by $W \approx 2\gamma_{\rm ph}(1 + \epsilon\gamma_{\rm ph})mc^2$ where $\epsilon = \phi/\phi_{\rm max} = n_1/n$ is the normalized potential or density perturbation associated with the wave and $\gamma_{\rm ph}$ is the Lorentz factor corresponding to the phase velocity $v_{\rm ph}$ of the wave. $\gamma_{\rm ph}$ is approximately ω/ω_p where ω is the laser frequency and ω_p is the plasma frequency. It is generally assumed that $v_{\rm ph} = v_g$, where $v_g = c(1 - \omega_p^2/\omega^2)^{1/2}$ is the linear group velocity of light in the plasma. Here we have only considered acceleration of the electron while it is in the focusing phase of the radial electric field since test particle calculations in ideal plasma waves have shown that electrons injected into defocusing regions are deflected out of the wave as they are accelerated [9]. The dephasing distance is obtained by simply calculating the distance it takes a particle moving at c to move ahead of the wave moving at $v_{\rm ph}$, by $\frac{1}{4}$ of the plasma wavelength, $\lambda_p/4$. This gives a dephasing distance, $L = \pi\gamma_{\rm ph}^2/k_p$ where $k_p = \omega_p/c$.

The above estimates for W and L are only valid for small ϵ and constant $v_{\rm ph}$ plasma waves as seen in self-consistent particle-in-cell (PIC) simulations of plasma beat-wave and laser wake field accelerators [10]. However, for extremely nonlinear plasma waves there are many mechanisms including frequency shifts [11], relativistic effects [12–14], pulse shape and time evolution of the driver [15], incoherent plasma wave dynamics [16], and self-generated focusing fields [17] that can lead to energy gains greater or less than the linear dephasing limit.

The experiments reported here were carried out at the Central Laser Facility at the Rutherford Appleton Laboratory with the 1.053 μm laser system Vulcan [18]. The laser was able to provide up to 20 J in a nominally 1 ps laser pulse. The beam could be focused to a 20 μm diameter spot using an $f/4.5$ off axis-paraboloid mirror onto the edge of a 4 mm diameter laminar plume of helium gas from a supersonic gas jet to produce a tunnel-ionized plasma. The Rayleigh range $2Z_R$, defined as the distance over which the laser intensity is greater than half of its peak value, is $\approx$700 μm. The typical laser intensity in vacuum was 6×10^{18} W/cm^2 corresponding to an $a_0 \approx 2$. Collective Thomson scattering of a 0.53 μm, 20 ps long probe beam was used to image the spatial extent of the Raman forward scattering (RFS) driven plasma wave. The 1 cm diameter probe beam was at 104° with respect to the pump beam and contained typically 5 mJ of energy. Photons scattered at $3.4° \pm 1.9°$ from the probe beam axis were imaged onto the slit of an imaging spectrometer. The spatial resolution of the Thomson scattering imaging system was about 150 μm.

The electrons accelerated in the interaction region passed through an $f/100$ collimator and were dispersed using a Brown and Buechner spectrometer [19]. The plasma wave was excited by an intense ($a_0 > 1$), short laser pulse via the RFS instability [20,21] and wake formation from the distortion of the leading edge of the pulse. Here $a_0 = eE_0/m\omega_0 c$ is the normalized oscillatory velocity of the electron in the laser field E_0 of frequency ω_0. RFS is the decay of an electromagnetic wave (ω_0, k_0) into a relativistic plasma wave (ω_p, k_p) and two forward propagating electromagnetic waves, anti-Stokes and Stokes $(\omega_0 \pm \omega_p, k_0 \pm k_p)$.

In Fig. 1(a) we show a frequency resolved image of the plasma wave, when the pump is focused at the edge of the gas jet plume ($x = -2$ mm), obtained by Thomson scattering of the probe beam. The Thomson scattering geometry is k matched to plasma wave modes centered around $\mathbf{k} = k_p\hat{\mathbf{x}} \pm k_\perp\hat{\mathbf{y}}$, where $k_\perp/k_p \sim 1$, k_p is the wave vector of the relativistic plasma wave, and $\hat{\mathbf{x}}$ and $\hat{\mathbf{y}}$ are the unit vectors. Note that while each mode by itself is nonrelativistic, their superposition is a relativistic plasma wave with transverse spatial structure which comes about because the laser spot size is on the order of a plasma wavelength. The scattered light appears as a wavelength shifted feature at $\Delta\lambda \approx -34$ nm. This shift is identical to the shift associated with the anti-Stokes satellite that is observed in the transmitted beam. From this shift we infer an effective plasma density [22] of 1.4×10^{19} cm^{-3} (gas jet backing pressure of 21 bars) which gives $\gamma_{\rm ph} = 8.5$ and a dephasing distance $L \approx 0.32$ mm. The observed uniformity of the frequency shift indicates that within the 50 Å frequency resolution of the detection system the plasma density is uniform throughout the length of the plasma wave. As indicated in the inset to Fig. 1(a), the wave amplitude is greater than $\frac{1}{3}$ its maximum value over 0.6 mm which is approximately one Rayleigh range. Since the laser power for this particular shot (20 TW) was far above the critical power for relativistic self-focusing [23] one might expect the plasma wave to exist over lengths much greater than a Rayleigh range. However, the length over which a plasma wave is excited depends critically on where in the gas the laser is focused. Under other focusing conditions, much longer plasma waves were observed, including one extending across the entire 4 mm length of the gas jet [24]. Such shots did not produce the highest energy electrons (>50 MeV), however, possibly because of the observed effective density inhomogeneity across the gas jet.

It is difficult to obtain an absolute estimate of the amplitude of the plasma wave from the scattered power because of large uncertainties in estimating the transverse dimension and time duration of the plasma wave. However, on some shots the second harmonic of the plasma wave is also seen in the Thomson scattered spectrum. From these shots, based on harmonic ratios [25], we estimate the amplitude of the wave to be $n_1/n \approx 40 \pm 20\%$.

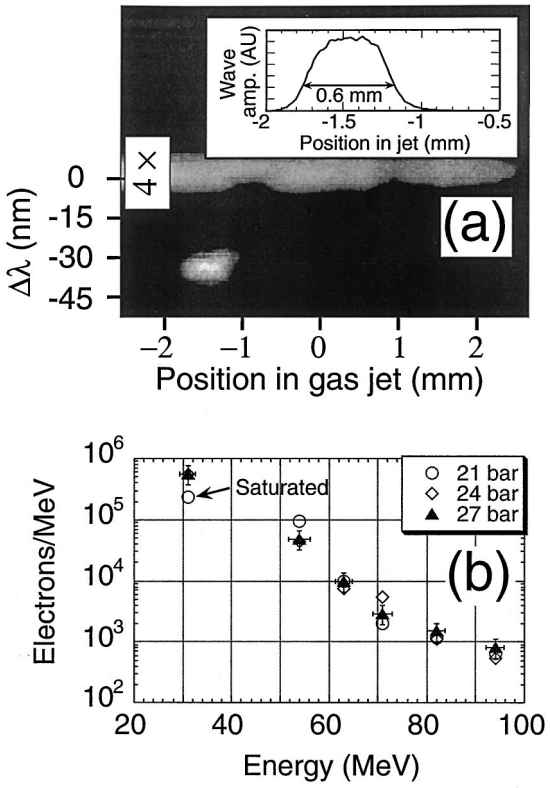

FIG. 1. (a) Thomson scattered spectrum vs distance along the gas jet indicating the spatial extent of the relativistic plasma wave. Position zero is the center of the 4 mm diameter gas jet. The laser propagates from left to right and is focused at -2.0 mm. The stray light at $\Delta\lambda = 0$ has been attenuated by 4. The gas jet backing pressure was 21 bars. Wave amplitude vs position is shown in inset. (b) The electron spectra measured in the forward $f/100$ cone angle at three backing pressures. The horizontal error bars indicate the range of energies incident on each detector as well as taking into account possible positioning errors. The vertical error bars reflect the uncertainty in detector sensitivity. The signal to noise ratio is independent of this error.

In Fig. 1(b) we show the electron spectrum measured between 30 and 100 MeV on 3 different laser shots in which the gas pressure was varied from 21 to 27 bars. The spectra show a monotonically falling electron distribution function. The signal to noise ratio is 100 at 32 MeV dropping to about 2 at 94 MeV. Clearly, all the electrons with energies greater than 55 MeV have exceeded the dephasing limit even for the lowest density of 1.4×10^{19} cm^{-3}. Furthermore, for the highest density shot ($n_{\rm eff} \approx 2 \times 10^{19}$ cm^{-3} at 27 bars $\Rightarrow \gamma_{\rm ph} = 7$), the spectrum extends beyond 74 MeV which is the energy an electron would have even if it were to survive the full $\lambda_p/2$ accelerating phase of the plasma wave. It could be supposed that the increased acceleration must be due to an effective decrease in the plasma frequency either because of ponderomotive blowout or a relativistic increase in the electron mass, since both effects should be prevalent at such high incident laser intensities. However, Fig. 1(a)

shows that the experimentally measured effective plasma frequency is nearly constant throughout the length of the plasma wave. It is therefore necessary to resort to PIC simulations to clarify the observed acceleration.

To show that the Thomson scattering data is consistent with the observation of 94 MeV electrons, we integrate the amplitude of the accelerating electric field over the length of the plasma wave shown in Fig. 1(a) using the data shown in the inset. This gives the energy gained by an electron that traverses the entire length of the plasma wave without ever slipping out of the peak accelerating phase. Using the most liberal estimate of the peak field ($\epsilon = 0.6$), such a particle would gain 120 MeV. Thus, to account for the observation of 94 MeV electrons, acceleration must occur over nearly the whole length of the plasma wave, which is twice the dephasing length mentioned earlier.

The fully relativistic code PEGASUS [15] uses a 2D Cartesian grid which moves at the speed of light. In this simulation a 1 μm, 600 fs (FWHM) diffraction limited pulse with a peak vacuum intensity of 5×10^{18} W/cm^2 and a 20 μm diameter spot size is propagated through a 1 mm slab of 1.4×10^{19} cm^{-3} plasma. The plasma begins at $x = 0$ mm. The ions are modeled as a fixed uniform neutralizing background. The results from this code [15,26] have been shown to be in agreement with observables from this and another [27] experiment. As discussed elsewhere [15], the laser pulse undergoes a complex spatial-temporal evolution of Raman scattering (back, side, forward), and self-focusing followed by filamentation. The front of the pulse etches away from Raman sidescatter leading to a deformed laser pulse envelope. This deformation generates a wake which seeds Raman forward scattering. The phase velocity of the wake as computed from $v_{\rm ph} = v_g$ corresponds for our simulation parameters to $\gamma_{\rm ph}^2 = 70$. However, the simulation results show that the phase velocity of the first few wavelengths of the wake initially correspond to $\gamma_{\rm ph}^2 = 50$. In other words, $v_{\rm ph} \neq v_g$. We believe this discrepancy to be real, probably due to the reduction in phase velocity of the wake caused by the etching away of the front of the laser pulse [13]. Based on the value $\gamma_{\rm ph}^2 = 50$ one would expect the energy gain of particles (once trapped) to cease because of dephasing after 0.22 mm.

For this simulation, the accelerating plasma wave breaks after the leading edge of the pulse has propagated approximately 0.4 mm into the plasma slab. At this point the maximum normalized amplitude of the accelerating field is quite close to $\epsilon = 1$. Once wave breaking occurs and a significant number of electrons are self-trapped the wave amplitude is reduced to $0.25 < \epsilon < 0.65$ because of beam loading. In other words the trapped electrons are accelerated at an average ϵ of less than 1. This is illustrated in Fig. 2(a) where we plot the normalized accelerating field on axis, E_x, and the normalized longitudinal momentum, P_x, of electrons above 4 MeV vs $x - ct$ for the plasma wave buckets containing the most energetic trapped particles. The front of the laser pulse is at $x - ct = 0$, while x is held fixed at 1 mm. Although not shown here, prior to wave breaking, only a few particles are trapped in these buckets, and their energies are limited to about 5 MeV. As can be seen in Fig. 2(a) the electrons are accelerated up to 80 MeV while E_x is much less than 1 for all the buckets. The peak electron energies are therefore beyond the linear dephasing estimate of $2\epsilon\gamma_{\rm ph}^2 mc^2$, which even for an ϵ of 0.65 and $\gamma_{\rm ph}^2$ of 50 gives $W = 42$ MeV. Furthermore, it is clear that due to beam loading the plasma wave has lost its coherence (i.e., its wavelength is not constant) and that some particles are still at peak accelerating regions while others are at peak decelerating regions. This illustrates that once wave breaking occurs the plasma wave's phase velocity is not given by the simple theory.

We have observed in this and several other simulations that within the laser pulse envelope, particles trapped in the later buckets are the ones that gain the highest energies [26] even though the wave amplitude is neither the largest nor sinusoidal there. We conjecture that as

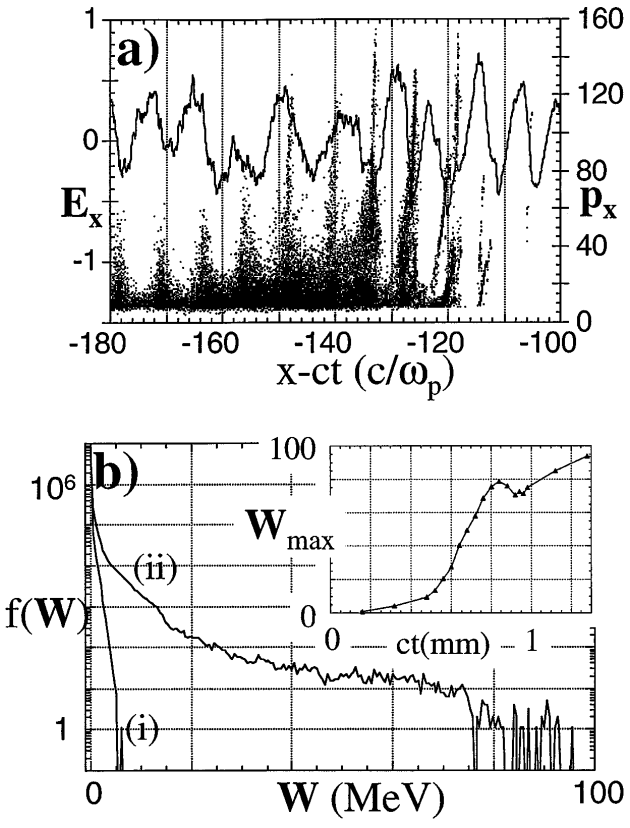

FIG. 2. (a) The normalized electric field E_x (lines) in units of $mc\omega_p/e$ and the normalized electron longitudinal momentum P_x (dots) in units of mc vs distance from the leading edge of the laser pulse ($x - ct$) in units of c/ω_p fixing x at 1 mm into the plasma. (b) Maximum electron energy $W_{\rm max}$ in MeV vs ct (inset) and the electron distribution functions at $ct = 0.4$ mm (i) and 1.3 mm (ii).

the particles trapped in the earlier buckets gain energy, the wake produced by them similarly accelerates. The total electric field is the superposition of the original wave field and the wake field induced by the trapped particles. This total field consequently not only becomes incoherent because of the large energy spread of the trapped particles in the earlier buckets, but the effective phase velocity of this field increases. This appears to cause some particles in the later buckets to gain energies higher than the linear dephasing limit.

To further illustrate that some of the trapped particles have gone beyond the simple dephasing estimate, we plot the energy of the most energetic electrons vs ct in the inset of Fig. 2(b). We see that in an average sense the electrons with maximum energy at any given ct are accelerated at a nearly constant rate from $ct \approx 0.5$ to 0.85 mm. If simple dephasing were occurring, then the rate would not be constant and, in fact, particles would begin to lose energy beyond the dephasing length of 0.22 mm. Over this distance the average E_x is 0.65 which corresponds to a gradient of $\approx$2.4 GeV/cm. Note further that after 0.85 mm the peak electron energy dips but then begins to increase further to a peak value of $\approx$95 MeV demonstrating the turbulent nature of acceleration. Since the plasma slab is only 1 mm thick, electron energy gain beyond $ct = 1$ mm is due to accelerating buckets in the back of the laser pulse since the front of the pulse has exited the plasma. Following wave breaking, which occurs at $ct = 0.4$ mm, most of this energy gain occurs in $\approx$0.6 mm. This is consistent with the measurement of the spatial profile of the plasma wave shown in the inset of Fig. 1(a).

To make further comparison with the experiment, we plot the electron distribution function for electrons within an $f/32$ collection angle. (The experiment used $f/100$.) The different curves correspond to ct of 0.4 mm (i) and 1.3 mm (ii), respectively. As stated before, a few high energy electrons are generated until $\approx$0.4 mm, and after that both the maximum energy and number of electrons increase with propagation distance. While the maximum energies observed are very similar in the experiment and the simulation, there are relatively greater numbers of lower energy electrons observed in the experiment.

In conclusion, we have measured the spatial extent of the relativistic plasma wave and the spectrum of the accelerated electrons by such a wave simultaneously. The maximum observed energies are greater than that expected from the linear dephasing limit for preinjected electrons.

This work was supported by a grant from EPSRC and EU at Imperial College, and by U.S. DOE Grants No. DE-FG03-92ER40727 and No. DE-FG03-98DP00211, and NSF Grant No. DMS-9722121 at UCLA.

[1] C. Joshi *et al.*, Nature (London) **311**, 525 (1984).
[2] C. E. Clayton *et al.*, Phys. Rev. Lett. **70**, 37 (1993).
[3] Y. Kitagawa *et al.*, Phys. Rev. Lett. **68**, 48 (1992); C. Joshi *et al.*, Phys. Rev. Lett. **47**, 1285 (1981).
[4] M. Everett *et al.*, Nature (London) **74**, 1355 (1995).
[5] A. Modena *et al.*, Nature (London) **377**, 608 (1995).
[6] Wagner *et al.*, Phys. Rev. Lett. **78**, 3125 (1997); A. Ting *et al.*, Phys. Plasmas **4**, 1889 (1997).
[7] D. Umstadter *et al.*, Science **76**, 2073 (1996).
[8] T. Tajima and J. M. Dawson, Phys. Rev. Lett. **43**, 267 (1979).
[9] R. Williams *et al.*, Laser Part. Beams **8**, 427 (1990).
[10] K. C. Tzeng *et al.* (to be published).
[11] M. N. Rosenbluth and C. S. Liu, Phys. Rev. Lett. **29**, 701 (1972); W. B. Mori, IEEE Trans. Plasma Sci. **PS-15**, 88 (1992).
[12] E. Esaray *et al.*, IEEE Trans. Plasma Sci. **PS-24**, 252 (1996).
[13] C. Decker and W. B. Mori, Phys. Rev. E **51**, 1364 (1995).
[14] T. Katsouleas and W. B. Mori, Phys. Rev. Lett. **61**, 90 (1988).
[15] K. C. Tzeng and W. B. Mori, Phys. Rev. Lett. **76**, 3332 (1996).
[16] D. W. Forslund *et al.*, Phys. Rev. Lett. **54**, 558 (1985).
[17] L. Gorbunov *et al.*, Phys. Rev. Lett. **76**, 2495 (1996).
[18] C. N. Danson *et al.*, Opt. Commun. **103**, 392 (1993).
[19] C. E. Clayton *et al.*, in *Proceedings of the 1995 Particle Accelerator Conference, Dallas, TX, 1995* (IEEE, Piscataway, NJ, 1996), Vol. 1, p. 637.
[20] W. B. Mori *et al.*, Phys. Rev. Lett. **72**, 1482 (1994).
[21] D. W. Forslund *et al.*, Phys. Fluids **18**, 1002 (1975).
[22] The effective plasma density is $n_{\text{eff}} = n/\gamma$ where γ is the relativistic Lorentz factor associated with the electrons as they quiver in the laser field. The relativistically correct plasma frequency is then given by $\omega_p^2 = 4\pi n_{\text{eff}} e^2/m$.
[23] P. Sprangle *et al.*, Phys. Rev. Lett. **73**, 3544 (1994); P. Sprangle *et al.*, *ibid.* **69**, 2200 (1992).
[24] C. E. Clayton *et al.*, Report No. UCLA PPG No. 1578 (to be published).
[25] A. Lal *et al.*, Phys. Plasmas **4**, 1434 (1997).
[26] K. C. Tzeng *et al.*, Report No. UCLA PPG No. 1577 (to be published).
[27] C. Coverdale *et al.*, Phys. Rev. Lett. **74**, 4659 (1995).